Radiative corrections to off-shell gauge-boson pair production[*]

WIM BEENAKKER

Instituut–Lorentz, University of Leiden, NL–2300 RA Leiden, The Netherlands

AND

ANSGAR DENNER

Paul Scherrer Institut, CH–5232 Villigen PSI, Switzerland

We give an overview of the problems and developments associated with the calculation of radiative corrections to off-shell gauge-boson pair production in e^+e^- collisions.

PACS numbers: 12.15.Lk, 13.40.Ks, 14.70.Fm, 14.70.Hp

1. Introduction

In recent years we have grown increasingly accustomed to the great success of the Standard Model (SM) of electroweak interactions. However, up to now only a relatively restricted sector of the SM has been checked. The Yang–Mills character of the gauge-boson self-interactions and the Higgs mechanism of mass generation still await conclusive confirmation. This leaves ample of room for interesting physics at upcoming collider experiments, either within or outside the SM. If any physics beyond the SM exists, it will reveal itself in the production of new particles (direct signals) or in deviations in the interactions between the SM particles (indirect signals).

Reactions that involve the production and subsequent decay of pairs of unstable gauge bosons ($e^+e^- \to V_1 V_2 \to 4f + n\gamma$) constitute powerful search tools for such indirect signals. In this context, the limelight is presently on the production of pairs of W bosons at LEP2, the second stage of the LEP program. With energies above the nominal W-pair-production threshold,

---

[*] Talks presented at the Zeuthen Workshop on Elementary Particle Theory: "Loops and Legs in Gauge Theories", Rheinsberg, Germany, April 19 – 24, 1998.

LEP2 offers a twofold possibility of testing the SM. First of all, it allows a precise direct measurement of the W-boson mass (M_{W}) with an envisaged precision of $\Delta M_{\mathrm{W}} = 40-50\,\mathrm{MeV}$ [1]. By combining this precise measurement of M_{W} with the high-precision data on α, G_μ, and M_{Z}, the mass of the top quark can be calculated within the SM as a function of the Higgs-boson mass M_{H} and the strong coupling α_s [2]. The so-obtained top-quark mass can then be confronted with the direct bounds from the Tevatron and the indirect ones from the precision measurements at LEP1/SLC. In this way improved limits on M_{H} can be obtained. On the other hand, LEP2 can provide information on the structure of the triple gauge-boson couplings (TGC) [3]. These couplings appear at tree level in LEP2 processes like $\mathrm{e}^+\mathrm{e}^- \to 4f$ or $\mathrm{e}^+\mathrm{e}^- \to \nu_{\mathrm{e}}\bar{\nu}_{\mathrm{e}}\gamma$, in contrast to LEP1 observables where they only entered through loop corrections. At LEP2 one hopes to determine the TGC with a relative precision of $\sim 10\%$ with respect to the SM couplings.

At a high-energy linear collider (LC), with its envisaged energy in the range $500-2000\,\mathrm{GeV}$, one can go one step further. Apart from TGC studies well below the per-cent level, the high LC energies also open the possibility of studying quartic gauge-boson couplings in reactions like $\mathrm{e}^+\mathrm{e}^- \to 6f$ or $\gamma\gamma \to 4f$, thereby entering the realm of the symmetry-breaking mechanism [4]. On top of that one can look for signs of a strongly-interacting symmetry-breaking sector (i.e. resonances or phase shifts), by studying longitudinal gauge-boson interactions in $\mathrm{e}^+\mathrm{e}^- \to 4f$, $6f$ and $\gamma\gamma \to 4f$.

In order to successfully achieve the above-mentioned physics goals, a very accurate knowledge of the SM predictions for the various observables is mandatory. This requires a proper understanding of radiative corrections as well as a proper treatment of finite-width effects. In the next sections we address these two topics in detail.

2. Gauge-invariant treatment of unstable gauge bosons

2.1. Lowest order

The above-described physics issues all involve an investigation of processes with photons and/or fermions in the initial and final state and unstable gauge bosons as intermediate particles. If complete sets of graphs contributing to a given process are taken into account, the associated matrix elements are in principle gauge-invariant, i.e. they are independent of gauge fixing and respect Ward identities. However, the gauge bosons that appear as intermediate particles can give rise to poles $1/(p_V^2 - M_V^2)$ in physical observables if they are treated as stable particles. This can be cured by introducing the finite decay width. In field theory, such widths arise

naturally from the imaginary parts of higher-order diagrams describing the gauge-boson self-energies, resummed to all orders. However, in doing a Dyson summation of self-energy graphs, we are singling out only a very limited subset of all possible higher-order diagrams. It is therefore not surprising that one often ends up with a result that violates Ward identities and/or retains some gauge dependence resulting from incomplete higher-order contributions.

Until a few years ago two approaches were popular in the construction of lowest-order LEP2/LC Monte Carlo generators. The first one, the so-called "fixed-width scheme", involves the systematic replacement $1/(p_V^2 - M_V^2) \rightarrow 1/(p_V^2 - M_V^2 + iM_V\Gamma_V)$, where Γ_V denotes the physical width of the gauge boson with mass M_V and momentum p_V. Since in perturbation theory the propagator for space-like momenta does not develop an imaginary part, the introduction of a finite width also for $p_V^2 < 0$ has no physical motivation and in fact violates unitarity, i.e. the cutting equations. This can be cured by using a running width $iM_V\Gamma_V(p_V^2)$ instead of the constant one $iM_V\Gamma_V$ ("running-width scheme").

As in general the resonant diagrams are not gauge-invariant by themselves, the introduction of a constant or running width destroys gauge invariance. At this point the question arises whether the gauge-breaking terms are numerically relevant or not. After all, the gauge breaking is caused by the finite decay width and is, as such, in principle suppressed by powers of Γ_V/M_V. For LEP1 observables we know that gauge breaking can be negligible for all practical purposes. However, the presence of small scales can amplify the gauge-breaking terms. This is for instance the case for almost collinear space-like photons [5] or longitudinal gauge bosons (V_L) at high energies [6], involving scales of $\mathcal{O}(p_B^2/E_B^2)$ for $B = \gamma, V_L$. The former plays an important role in TGC studies in the reaction $e^+e^- \rightarrow e^-\bar{\nu}_e u\bar{d}$, where the electron may emit a virtual photon with p_γ^2 as small as m_e^2. The latter determines the high-energy behaviour of the generic reaction $e^+e^- \rightarrow 4f$. In these situations the external current coupled to the photon or to the longitudinal gauge boson becomes approximately proportional to p_B. Sensible theoretical predictions, with a proper dependence on p_γ^2 and a proper high-energy behaviour, are only possible if the amplitudes with external currents replaced by the corresponding gauge-boson momenta fulfill appropriate Ward identities.

In order to substantiate these statements, a truly gauge-invariant scheme is needed. It should be stressed, however, that any such scheme is arbitrary to a greater or lesser extent: since the Dyson summation must necessarily be taken to all orders of perturbation theory, and we are not able to compute the complete set of *all* Feynman diagrams to *all* orders, the various schemes differ even if they lead to formally gauge-invariant results. Bearing

this in mind, we need besides gauge invariance some physical motivation for choosing a particular scheme. In this context two options can be mentioned. The first option is the so-called "pole scheme" [7]. In this scheme one decomposes the complete amplitude by expanding around the poles. As the physically observable residues of the poles are gauge-invariant, gauge invariance is not broken if the finite width is taken into account in the pole terms $\propto 1/(p_V^2 - M_V^2)$. It should be noted that there is no unique definition of these residues. Their calculation involves a mapping of off-shell matrix elements with off-shell kinematics on on-resonance matrix elements with restricted kinematics. The restricted kinematics, however, is not unambiguously fixed. After all, it contains more than just the invariant masses of the unstable particles and one has to specify the variables that have to be kept fixed when determining the residues. The resulting implementation dependence manifests itself in differences of subleading nature, e.g. $\mathcal{O}(\Gamma_V/M_V)$ suppressed deviations in the leading pole-scheme residue. In particular near phase-space boundaries, like thresholds, the implementation differences can take on noticeable proportions.

We roughly sketch the pole-scheme method for a single unstable particle. The Dyson resummed lowest-order matrix element is given by

$$
\begin{aligned}
\mathcal{M}^\infty &= \frac{W(p_V^2,\omega)}{p_V^2 - M_V^2} \sum_{n=0}^{\infty} \left(\frac{\Sigma_V(p_V^2)}{p_V^2 - M_V^2} \right)^n = \frac{W(p_V^2,\omega)}{p_V^2 - M_V^2 - \Sigma_V(p_V^2)} \\
&= \frac{W(M^2,\omega)}{p_V^2 - M^2} \frac{1}{Z(M^2)} + \left[\frac{W(p_V^2,\omega)}{p_V^2 - M_V^2 - \Sigma_V(p_V^2)} - \frac{W(M^2,\omega)}{p_V^2 - M^2} \frac{1}{Z(M^2)} \right],
\end{aligned}
\tag{1}
$$

where $\Sigma_V(p_V^2)$ is the self-energy of the unstable particle, M^2 is the pole in the complex p_V^2 plane, and $Z(M^2)$ is the wave-function factor: $M^2 - M_V^2 - \Sigma_V(M^2) = 0$ and $Z(M^2) = 1 - \Sigma_V'(M^2)$. The first term in the last expression of (1) represents the single-pole residue, which is closely related to on-shell production and decay of the unstable particle. The argument ω denotes the dependence on the other variables, i.e. the implementation dependence. The second term has no pole and can be expanded in powers of $p_V^2 - M^2$.

The second option is based on the philosophy of trying to determine and include the minimal set of Feynman diagrams that is necessary for compensating the gauge violation caused by the self-energy graphs. This is obviously the theoretically most satisfying solution, but it may cause an increase in the complexity of the matrix elements and a consequent slowing down of the numerical calculations. For the gauge bosons we are guided by the observation that the lowest-order decay widths are exclusively given by the imaginary parts of the fermion loops in the one-loop self-energies. It

is therefore natural to perform a Dyson summation of these fermionic one-loop self-energies and to include the other possible one-particle-irreducible fermionic one-loop corrections ("fermion-loop scheme") [5, 6]. For the LEP2 process $e^+e^- \to 4f$ this amounts to adding the fermionic corrections to the triple gauge-boson vertex. The complete set of fermionic contributions forms a gauge-independent subset and obeys all Ward identities exactly, even with resummed propagators [6].

Having two gauge-invariant calculational schemes to compare with, we can now have a closer look at the ever-popular fixed- and running-width schemes. The running-width scheme violates electromagnetic and SU(2) gauge invariance already in $e^+e^- \to 4f$ and is found to produce completely unreliable results [5, 6]. Within the fixed-width scheme electromagnetic gauge invariance is preserved in $e^+e^- \to 4f$ for massless external particles, eliminating problems with almost collinear space-like photons. This is indeed confirmed by the numerical comparison in Refs. [5, 6]. In more general reactions, like $e^+e^- \to 4f\gamma$, electromagnetic gauge invariance is broken. Owing to the presence of non-transverse W-boson contributions, electromagnetic gauge invariance in $e^+e^- \to 4f\gamma$ can be achieved only if the process $e^+e^- \to 4f$ is SU(2) gauge-invariant. At high energies ($E_V \gg M_V$) the fixed-width scheme in general violates SU(2) gauge invariance by terms of the order $M_V\Gamma_V/E_V^2$ [6]. In matrix elements for physical processes the gauge-invariance-violating terms are enhanced by a factor E_V/M_V for each effectively longitudinal gauge boson. The process $e^+e^- \to 4f$ involves at most two longitudinal gauge bosons, such that the SU(2) gauge violation is suppressed by Γ_V/M_V at the matrix-element level. Therefore, the high-energy behaviour of the cross-section in the fixed-width scheme is consistent with unitarity, which is confirmed by the numerical comparison in Ref. [6]. However, our argument implies a bad high-energy behaviour for processes with more intermediate (longitudinal) gauge bosons, like longitudinal gauge-boson scattering in $e^+e^- \to 6f$.[1]

2.2. Radiative corrections

The implementation of radiative corrections adds an additional level of complexity by the sheer number of contributions ($10^3 - 10^4$) that have to be evaluated.

---

[1] A fixed-width scheme that preserves electromagnetic and SU(2) gauge invariance is only possible if one uses *one* complex gauge-boson mass, everywhere. Consequently, the complex W and Z masses have to be related by $M_W^2 - iM_W\Gamma_W = c_w^2(M_Z^2 - iM_Z\Gamma_Z)$, leading to a relation between the decay widths that is not supported by experiment.

By employing the fermion-loop scheme all one-particle-irreducible fermionic one-loop corrections can be embedded in the tree-level matrix elements. This results in running couplings, propagator functions, vertex functions, etc. However, there is still the question about the bosonic corrections. A large part of these bosonic corrections, as e.g. the leading QED corrections, factorize and can be treated by means of a convolution, using the fermion-loop-improved cross-sections in the integration kernels. This allows the inclusion of higher-order QED corrections and soft-photon exponentiation. In this way various important effects can be covered, as e.g. the large negative soft-photon corrections near the nominal W-pair threshold, the distortion of angular distributions as a result of hard-photon boost effects, and the average energy loss due to radiated photons [2, 8]. Nevertheless, the remaining bosonic corrections can be large, especially at high energies [2, 8, 9].

In order to include these corrections one might attempt to extend the fermion-loop scheme. In the context of the background-field method [10] a Dyson summation of one-loop bosonic self-energies can be performed without violating the Ward identities [11]. However, the resulting matrix elements depend on the quantum gauge parameter at the loop level that is not completely taken into account. As mentioned before, the perturbation series has to be truncated; in that sense the dependence on the quantum gauge parameter could be viewed as a parametrization of the associated ambiguity.

As an additional complication for such Dyson-summation techniques, we mention that a consistent calculation of the radiative corrections involves also the one-loop corrections to the decay widths. Since this requires the imaginary part of the two-loop self-energies, also other (imaginary parts of) two-loop corrections are needed to restore gauge invariance. An efficient way of overcoming this complication is still under investigation.

As a more appealing and economic strategy we discuss in the next section how the radiative corrections can be calculated in an approximated pole-scheme expansion.

3. Radiative corrections in the double-pole approximation

The presently most favoured framework for evaluating the radiative corrections to resonance-pair-production processes, like W- and Z-pair production, involves the so-called double-pole approximation (DPA). This approximation restricts the complete pole-scheme expansion to the term with the highest degree of resonance. In the case of W/Z-pair production only the double-pole residues are hence considered. The intrinsic error associated with this procedure is $\alpha \Gamma_V/(\pi M_V) \lesssim 0.1\%$, except far off resonance and
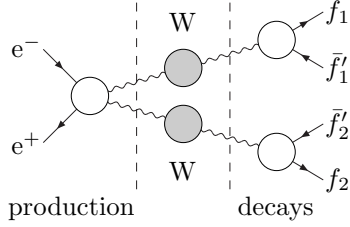
Fig. 1. The generic structure of the factorizable W-pair contributions. The shaded circles indicate the Breit–Wigner resonances.

close to phase-space boundaries where also the implementation dependence of the double-pole residues can lead to enhancement factors. For this reason the DPA is only valid a few Γ_V above the nominal (on-shell) gauge-boson-pair threshold.

In the DPA one can identify two types of contributions. One type comprises all diagrams that are strictly reducible at both unstable gauge-boson lines (see Fig. 1). These corrections are therefore called factorizable and can be attributed unambiguously either to the production of the gauge-boson pair or to one of the subsequent decays. The second type consists of all diagrams in which the production and/or decay subprocesses are not independent (see Fig. 2). We refer to these effects as non-factorizable corrections (NFC). In the DPA the NFC arise exclusively from the exchange or emission of photons with $E_\gamma \lesssim \mathcal{O}(\Gamma_V)$. Hard photons as well as other massive particles do not lead to double-resonant contributions.

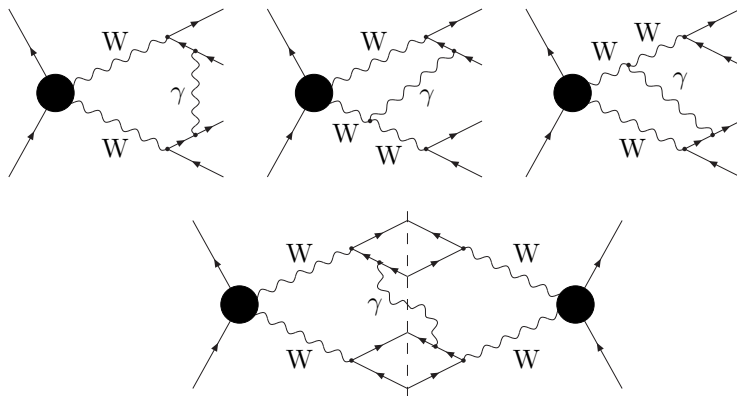In the case of photon emission from a W boson (see Fig. 3), the split-up

Fig. 2. Examples for virtual (top) and real (bottom) non-factorizable corrections to W-pair production.

between factorizable and non-factorizable corrections can be achieved with the help of a partial-fraction decomposition of the two W-boson propagators separated by the photon [12]:

$$\frac{1}{[p^2 - M^2][(p-k)^2 - M^2]} = \frac{1}{2(p \cdot k)} \left(\frac{1}{(p-k)^2 - M^2} - \frac{1}{p^2 - M^2} \right), \quad (2)$$

where $M^2 = M_{\mathrm{W}}^2 - \mathrm{i}M_{\mathrm{W}}\Gamma_{\mathrm{W}}$, k is the momentum of the emitted photon, and p is the momentum of the W boson before emission. In this way one obtains a sum of two resonant W-boson propagators multiplied by an ordinary on-shell eikonal factor. This decomposition allows a gauge-invariant split-up of the real-photon matrix element in terms of one contribution where the photon is effectively emitted from the production part, and another two where the photon is effectively emitted from one of the two decay parts. The squares of the three contributions can be identified as factorizable corrections, whereas the interference terms are of non-factorizable nature. The same type of split-up can be performed for the corresponding virtual corrections.

The factorizable corrections have the nice feature that they can be expressed in terms of corrections to on-shell subprocesses, i.e. the production of two on-shell gauge bosons $(V_1 V_2)$ and their subsequent on-shell decays. In this way the well-known on-shell radiative corrections to the production and decay of pairs of gauge bosons (see Ref. [8] and references therein) appear as basic building blocks of the factorizable corrections. For instance, for the virtual factorizable corrections in DPA one finds

$$\mathcal{M}_{\mathrm{f}} = \sum_{V \, \mathrm{pol.}} \frac{\mathcal{M}^{\mathrm{e^+e^-} \to V_1 V_2} \mathcal{M}^{V_1 \to f_1 \bar{f}_2} \mathcal{M}^{V_2 \to f_3 \bar{f}_4}}{(q_1^2 - M^2)(q_2^2 - M^2)}, \quad (3)$$

with $M^2 = M_V^2 - \mathrm{i}M_V\Gamma_V$ and $q_{1,2}^2$ the invariant masses squared of the bosons $V_{1,2}$. The off-shell character of the reaction is reflected by the occurrence of the two Breit–Wigner resonances.

3.1. Factorizable real-photon corrections in double-pole approximation

As indicated above, the factorizable real-photon corrections are characterized by their close relation to on-shell subprocesses. In this context three regimes for the photon energy play a role:

- for hard photons $[E_\gamma \gg \Gamma_V]$ the Breit–Wigner poles of the gauge-boson resonances before and after photon radiation (see s'_V and s_V in

Fig. 3) are well separated in phase space. This leads to three *distinct* regions of on-shell contributions, where the photon can be assigned unambiguously to the gauge-boson-pair-production subprocess or one of the two decays. Therefore, the double-pole residue can be expressed as the sum of the three on-shell contributions without increasing the intrinsic error of the DPA. Note that in the same way it is also possible to experimentally assign the photon to one of the subprocesses, since misassignment errors are suppressed.

- for "semi-soft" photons [$E_\gamma = \mathcal{O}(\Gamma_V)$] the Breit–Wigner poles are relatively close together in phase space, resulting in a substantial overlap of the line shapes. The assignment of the photon is now subject to larger errors, and the DPA has to be applied with caution.

- for soft photons [$E_\gamma \ll \Gamma_V$] the Breit–Wigner poles are on top of each other, resulting in a pole-scheme expansion that is identical to the one without the photon.

If the photon is integrated out, the reduction of the five-particle phase space to a four-particle one introduces a parametrization dependence. As we will see in the following, the size of the radiative corrections depends strongly on the choice of parametrization of the four-particle phase space.

When one produces two resonances, or one resonance and a stable particle, the line shape of such a resonance is measured from the invariant-mass distribution of its decay products. This has to be contrasted with the Z resonance at LEP1, which is defined as a function of the centre-of-mass energy squared. Depending on how one measures the invariant-mass distribution, different sources of Breit–Wigner distortions can be identified. At LEP1 such a distortion is caused by initial-state radiation (ISR) [13], but in our case also final-state radiation (FSR) can be responsible.

In Ref. [14] it has been shown that such a FSR-induced distortion is a general property of resonance-pair reactions, irrespective of the adopted scheme for implementing the finite-width effects. The only decisive factor for the distortion to take place is whether the virtuality of the unstable particle is defined with or without the radiated photon (see Fig. 3). Upon integration over the photon momentum, the former definition (s'_V) is free of large FSR effects from the V-decay system. It can only receive large corrections from the other (production or decay) stages of the process. The latter definition (s_V), however, does give rise to large FSR effects from the V-decay system. In contrast to the LEP1 case, where the ISR-corrected line shape receives contributions from effectively *lower* Z-boson virtualities, the s_V line shape receives contributions from effectively *higher* virtualities s'_V of the unstable particle. As was argued above, only sufficiently hard photons ($E_\gamma \gg \Gamma_V$)
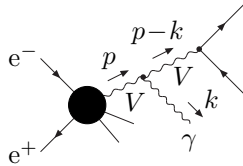
Fig. 3. Photon radiation from an unstable particle V. Virtualities: $s_V = (p - k)^2$ and $s'_V = p^2$.

can be properly assigned to one of the on-shell production or decay stages of the process in the DPA. For semi-soft photons $[E_\gamma = \mathcal{O}(\Gamma_V)]$, however, the assignment lacks a solid motivation and an invariant-mass definition in terms of the decay products without the photon seems more natural. As was pointed out in Ref. [14], exactly these semi-soft photons are responsible for the FSR-induced distortion effects. The hard FSR photons move the virtuality s'_V of the unstable particle far off resonance for near-resonance s_V values, resulting in a suppressed contribution to the s_V line shape. This picture fits in nicely with the negligible overlap of the three on-shell double-pole contributions for hard photons, discussed above.

The size of the FSR-induced distortion can be parametrized in terms of the shift in the peak position and the corresponding peak reduction factor with respect to the lowest-order line shape. These parameters depend strongly on the type of unstable particle and the precise experimental definition of the associated invariant mass.[2] The shift in the peak position generally amounts to several times $-10\,\mathrm{MeV}$. As extreme values we mention $-110\,\mathrm{MeV}$ for an unstable Z boson that decays as $\mathrm{Z} \to \mathrm{e^+e^-}$ and $-45\,\mathrm{MeV}$ for an unstable W boson that decays as $\mathrm{W} \to \mathrm{e}\nu_\mathrm{e}$, assuming no minimum opening angle between the leptons and the photon. The peak reduction factor lies in the range $0.95 - 0.75$. All this stresses the importance of a proper inclusion of FSR effects in the experimental method for extracting the gauge-boson masses from the reconstructed line shapes.

As an example we display in Fig. 4 the large FSR-induced distortion effects for the double-resonance toy process $\nu_\mu\bar\nu_\mu \to \mathrm{ZZ} \to \mathrm{e^-e^+}\nu_\tau\bar\nu_\tau$. Apart from being exactly calculable, this process is free of the usual gauge-invariance problems and it only receives QED corrections from the $\mathrm{Z} \to \mathrm{e^+e^-}$ decay. As such it is well suited for showing the salient features of FSR. Like at LEP1, the size of the $\mathcal{O}(\alpha)$ corrections indicates the need for a resummation of soft-photon effects. A justification of this can be found in the fact

---

[2] In realistic event-selection procedures a minimum opening angle between the decay products and the photon is required for a proper identification of all particles. This affects the integration range of the photon momentum and therefore the size of the distortion.
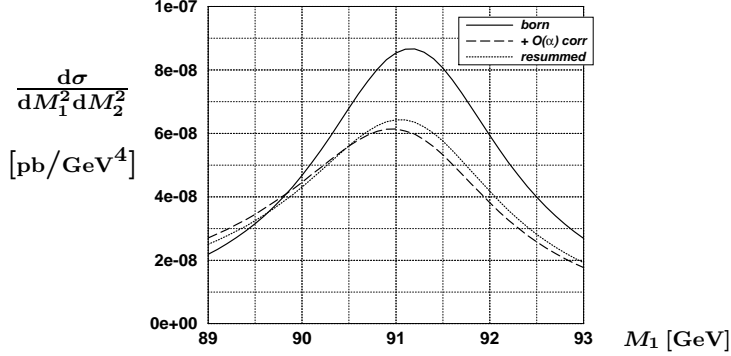
Fig. 4. The FSR-induced distortion of the line shape $d\sigma/(dM_1^2 \, dM_2^2)$ corresponding to the toy process $\nu_\mu\bar{\nu}_\mu \to ZZ \to e^-e^+\nu_\tau\bar{\nu}_\tau$ for $M_2 = M_Z$. Here M_1 and M_2 stand for the invariant masses of the e^-e^+ and $\nu_\tau\bar{\nu}_\tau$ pair, respectively. Centre-of-mass energy: $\sqrt{s} = 200\,\text{GeV}$. No minimum opening angle between the photon and $e^\pm$. Plot taken from Ref. [14].

that only semi-soft photons lead to the distortion. The resummation factor δ_{res} that multiplies the lowest-order double-invariant-mass distribution in Fig. 4 can be accurately approximated by

$$
\delta_{\text{res}} = \left(1 + \frac{3}{4}\beta\right) \int\limits_1^\infty d\zeta \, \beta \, (\zeta - 1)^{\beta-1} \, \frac{|D_Z(M_1^2)|^2}{|D_Z(\zeta M_1^2)|^2}
$$

$$
= \left(1 + \frac{3}{4}\beta\right) \frac{\pi\beta}{\sin(\pi\beta)} \, \text{Re}\left[\frac{iD_Z^*(M_1^2)}{M_Z\Gamma_Z} \left(\frac{D_Z(M_1^2)}{M_Z^2}\right)^\beta\right], \tag{4}
$$

with $\beta = (2\alpha/\pi)\,[\log(M_Z^2/m_e^2) - 1]$ and $D_Z(p^2) = p^2 - M_Z^2 + iM_Z\Gamma_Z$.[3] The fact that the FSR-corrected line shape receives contributions from effectively *higher* virtualities is reflected by the parameter ζ, which takes on values above unity. Apart from the inversion of ζ, the situation is the same as for ISR at LEP1. This analogy is also confirmed by simple rules of thumb for the peak position and peak reduction factor (cf. Refs. [14, 15]).

3.2. Non-factorizable corrections

---

[3] Equation (4) equally applies to other unstable particles and decay products, provided the definitions of the resonance parameters (M_Z, Γ_Z) and β are properly adjusted. For instance, a $W \to \mu\nu_\mu$ decay requires $M_Z \to M_W$, $\Gamma_Z \to \Gamma_W$, $m_e \to m_\mu$ and $\alpha \to \alpha/2$.
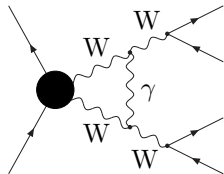
Fig. 5. Diagram contributing both to factorizable and non-factorizable corrections.

The NFC to gauge-boson pair production have been considered by several authors in recent years. First it was shown that the NFC vanish in inclusive quantities [16, 17], i.e. if the invariant masses of both gauge bosons are integrated out. The NFC to differential distributions in W-pair production were first calculated in Ref. [18], but the analytical results were given only in an implicit form and the numerical evaluation was restricted to a special phase-space configuration. Recently two groups have independently provided both the complete formulae and an adequate numerical evaluation for the leptonic final state [19, 20]. While these latter two calculations agree analytically and numerically, they deviate from the results of Ref. [18]. Subsequently, also numerical results for other final states in W-pair production and Z-pair production were investigated [21]. In the following, we discuss the results based on Refs. [19, 20, 21].

The manifestly non-factorizable diagrams (see Fig. 2 for examples) are not gauge-invariant. A gauge-invariant definition of the NFC can be given in different ways. One possibility, used in Ref. [19], is based on the fact that only soft and semi-soft photons contribute in the DPA. The associated matrix element can be written as a product of the lowest-order matrix element times conserved soft-photon currents, which can be decomposed into one production and two decay currents with the help of (2). The NFC are then defined as all interferences between the three currents.

A second definition [20] makes use of the gauge independence of the complete double-resonant corrections. The factorizable double-resonant corrections are given by the product of gauge-invariant on-shell matrix elements for gauge-boson pair production and gauge-boson decays, and the (transverse parts of the) gauge-boson propagators [see (3)]. Therefore, the double-resonant NFC can be defined by subtracting the double-resonant factorizable corrections from the complete double-resonant corrections. It turns out that both definitions are equivalent in the DPA and, for charged bosons, include parts of the diagram shown in Fig. 5 (cf. Ref. [16]).

Since only soft and semi-soft photons are relevant, each virtual diagram contributing to the NFC reduces to the corresponding lowest-order matrix element times a correction factor that involves besides kinematical variables

only a scalar integral. After evaluation of this scalar integral, an expansion of the residue around the poles at $p_V^2 = M_V^2$ can be performed. The constant finite width can be introduced either before integration or in the final result. It regularizes besides the resonant propagators also logarithms of the form $\log(p_V^2 - M_V^2)$.

The real-photon NFC can be calculated in a similar way. The integration region for the energy of the real photon can be extended to infinity without changing the result. However, when integrating over the photon momentum, the complete parametrization of phase space has to be specified [20]. In analogy to the factorizable corrections, also the real-photon NFC are not universal but depend on the choice of this parametrization, even in DPA. We follow the usual procedure and take the invariant masses of decay fermion pairs as independent variables.

After combining real and virtual contributions, the NFC yield a simple polarization-independent correction factor to the lowest-order cross-section:

$$d\sigma_{nf} = \delta_{nf}\, d\sigma_{Born}. \tag{5}$$

For the processes

$$e^+(p_+)+e^-(p_-) \;\to\; V_1(q_1)+V_2(q_2) \;\to\; f_1(k_1)+\bar{f}_2(k_2)+f_3(k_3)+\bar{f}_4(k_4), \tag{6}$$

with $V_1 V_2 = WW$ or ZZ, this factor can be written as [20]

$$\delta_{nf}(k_1, k_2; k_3, k_4) = \sum_{\substack{a=1,2 \\ b=3,4}} (-1)^{a+b+1}\, Q_a Q_b\, \frac{\alpha}{\pi}\, \mathrm{Re}\left\{\Delta(q_1, k_a; q_2, k_b)\right\}. \tag{7}$$

Here Q_i $(i = 1, 2, 3, 4)$ denotes the relative charge of fermion f_i and $q_1 = k_1 + k_2$, $q_2 = k_3 + k_4$ the momenta of the virtual bosons. Each term in the sum of (7) corresponds to the photon exchange between two specific final-state fermions that originate from different bosons. The function Δ is explicitly given in Ref. [20] and, in a different notation, in Ref. [19]. It has in DPA the important property: $(K_i \equiv q_i^2 - M_V^2 + iM_V\Gamma_V)$

$$\Delta + \Delta\Big|_{K_1 \to -K_1^*} + \Delta\Big|_{K_2 \to -K_2^*} + \Delta\Big|_{K_{1,2} \to -K_{1,2}^*} = 0. \tag{8}$$

The final result for the NFC has the following general features:

- Photon-exchange contributions between initial and final states cancel between virtual and real corrections, leaving behind the cross-talk between the two decay systems as only contributions. Consequently, the NFC are independent of the production angle of the gauge bosons and (7) is applicable to other initial states like $q\bar{q}$ or $\gamma\gamma$.

13

- The mass-singular logarithms that are present in individual contributions cancel, and the complete NFC are free of mass singularities. As a consequence, the typical order of magnitude of the NFC is $\alpha/\pi \sim 0.3\%$.

- Equation (8) implies that the NFC vanish if both virtual gauge bosons are on-shell. This leads to a suppression with respect to the factorizable corrections. For single-invariant-mass distributions the suppression factor is $(q_{1,2}^2 - M_V^2)/(M_V \Gamma_V)$. This is of order one in the vicinity of the resonance, i.e. for $q_{1,2}^2 - M_V^2 = \mathcal{O}(M_V \Gamma_V)$, ensuring that the NFC are genuine double-pole contributions.

- As can be seen from (8), the NFC vanish if both invariant masses are integrated over. Thus, they vanish for pure angular distributions and therefore have no impact on standard TGC studies.

- Finally, the NFC vanish at high energies. This can be easily illustrated by the result for the production of one stable and one unstable charged particle with equal masses, where the correction factor becomes [18]

$$\delta_{\mathrm{nf}} = -\alpha \, \frac{(1-\beta)^2}{\beta} \arctan\left(\frac{q^2 - M_V^2}{M_V \Gamma_V}\right) \quad \text{with} \quad \beta = \sqrt{1 - 4M_V^2/s}.$$

  This simple formula describes qualitatively also the realistic case of the single-invariant-mass distribution in the case of two unstable particles.

These features indicate that the NFC are less important than the factorizable corrections. But their actual relevance depends on the experimental accuracy and the observable under consideration.

We first consider the NFC to $e^+e^- \to WW \to 4f$. In Fig. 6 we show the NFC to the single-invariant-mass distribution $d\sigma/dM_1$ of the process $e^+e^- \to WW \to \nu_e e^+ e^- \bar{\nu}_e$ for various centre-of-mass energies. With $M_{1,2}$ we denote the invariant masses of the first and second fermion–antifermion pairs, respectively. The NFC are roughly 1% for $\sqrt{s} = 172\,\mathrm{GeV}$ and decrease fast with increasing energy. They distort the invariant-mass distribution and thus in principle influence the determination of the W-boson mass from the direct reconstruction of the decay products. The corresponding mass shift can be estimated by the displacement of the maximum of the single-invariant-mass distribution caused by the corrections shown in Fig. 6. This displacement turns out to be of the order of $1-2\,\mathrm{MeV}$, i.e. small compared to the LEP2 accuracy.

In Fig. 7 we compare the results for the single-invariant-mass distribution $d\sigma/dM_1$ for various final states, once calculated using the code of
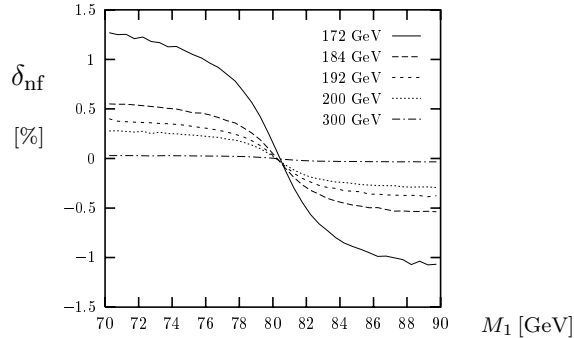
14

Fig. 6. Relative NFC to the single-invariant-mass distribution $\mathrm{d}\sigma/\mathrm{d}M_1$ for $\mathrm{e}^+\mathrm{e}^- \to \mathrm{WW} \to \nu_\mathrm{e}\mathrm{e}^+\mathrm{e}^-\bar{\nu}_\mathrm{e}$. Plot taken from Ref. [20].
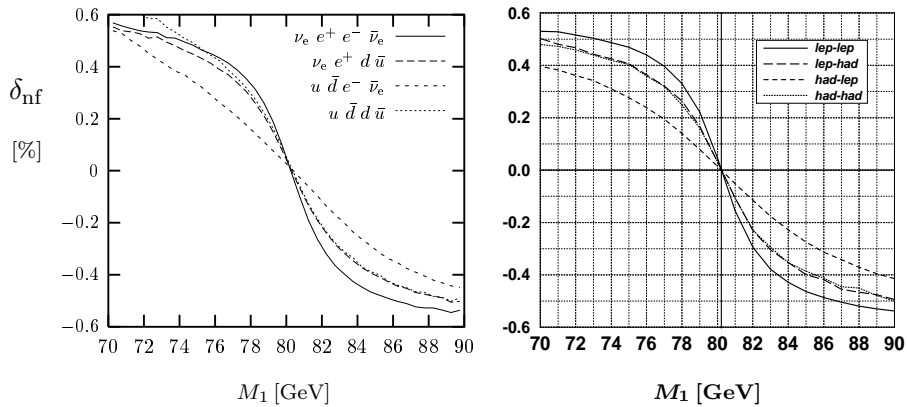
Fig. 7. Relative NFC to the single-invariant-mass distribution $\mathrm{d}\sigma/\mathrm{d}M_1$ for $\mathrm{e}^+\mathrm{e}^- \to \mathrm{WW} \to 4f$ with different final states. Left: results from Ref. [21]. Right: results based on Ref. [19]. Centre-of-mass energy: $\sqrt{s} = 184\,\mathrm{GeV}$.

Ref. [20] and once using the code of Ref. [19]. The NFC are similar for all final states. The NFC to the distribution $\mathrm{d}\sigma/\mathrm{d}M_2$ can be derived from the results for $\mathrm{d}\sigma/\mathrm{d}M_1$ by a CP transformation of the final state [21]. The results for the single-invariant-mass distributions agree very well between the two different calculations, in particular for large invariant masses and for invariant masses close to the W-boson mass, which dominate the cross-sections. The discrepancies for smaller invariant masses are of the order of the non-double-resonant corrections and are due to different implementations of the corrections. While in the numerical evaluations of Ref. [19] the phase space and the Born matrix element are taken entirely on-shell, these are taken off-shell in the evaluation of Refs. [20, 21].
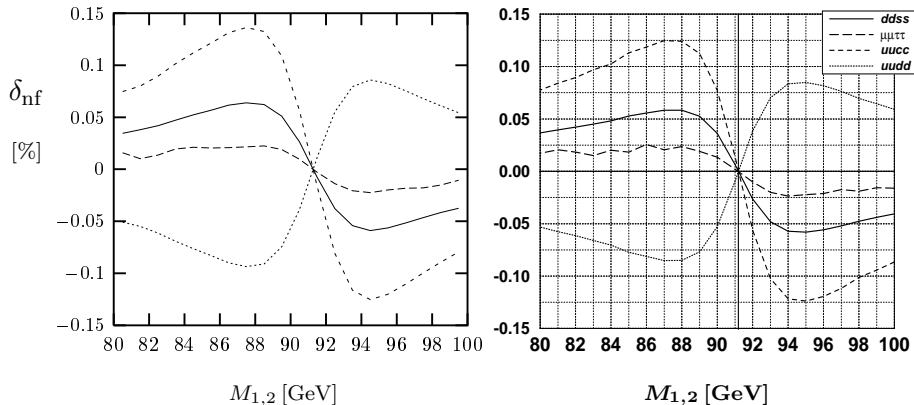
15

Fig. 8. Relative NFC to the single-invariant-mass distributions $d\sigma/dM_{1,2}$ for $e^+e^- \to ZZ \to 4f$ with different final states. Left: results from Ref. [21]. Right: results based on Ref. [19]. Centre-of-mass energy: $\sqrt{s} = 192\,\text{GeV}$.

Results for the dependence of the NFC on angles and energies of the final-state fermions can be found in Refs. [20, 21]. These NFC are typically of the order of one percent, i.e. somewhat larger than for the invariant-mass distributions. The largest effects of some per cent can be observed near the edges of phase space, where statistics is limited.

Next we consider the NFC to $e^+e^- \to ZZ \to 4f$. Figure 8 shows the NFC to the single-invariant-mass distribution $d\sigma/dM_1$, which is identical to $d\sigma/dM_2$. Again the results of Ref. [21] agree well with those based on Ref. [19]. For opposite signs of Q_1 and Q_3 the sign of the corrections is reversed with respect to $e^+e^- \to WW \to 4f$. The corrections by themselves are very small and phenomenologically unimportant. The smallness of these corrections results from the fact that δ_{nf} is symmetric in $k_1 \leftrightarrow k_2$ and $k_3 \leftrightarrow k_4$ after integration over the decay angles. For all observables that involve an integration over the phase space that respects this symmetry, the NFC are suppressed either by the charges or the vector couplings of the final-state fermions [21].

If the decay angles are not integrated out, this suppression does not apply. In fact, owing to the presence of four charged final-state fermions, the NFC to angular Z-pair distributions are enhanced with respect to the W-pair case by a factor of roughly four for purely leptonic final states, and can amount to up to 10% [21]. Note, however, that the cross-section for Z-pair production is only one tenth of the W-pair production cross-section.

4. Summary

16

For a gauge-invariant treatment of finite-width effects in lowest-order off-shell gauge-boson pair production two consistent schemes exist, i.e. the fermion-loop scheme and the pole scheme. For the calculation of the radiative corrections the latter scheme offers a promising framework in the form of the double-pole approximation. This approximation results in a split-up of the corrections in so-called factorizable and non-factorizable corrections. As far as the factorizable corrections are concerned, in particular the photonic ones are crucial for coming up with adequate theoretical predictions. While in this context the importance of initial-state radiation is evident and commonly acknowledged, also the Breit–Wigner distortions induced by final-state radiation should be taken into account properly. The non-factorizable corrections to W-pair and Z-pair production are small with respect to the experimental accuracy at LEP2. As a consequence, the factorizable corrections are sufficient for theoretical predictions for LEP2. The size of the non-factorizable corrections might, however, compete with the expected experimental accuracy at future linear e^+e^- colliders with higher luminosity.

REFERENCES

[1] Z. Kunszt *et al.*, in *Physics at LEP2*, eds. G. Altarelli, T. Sjöstrand and F. Zwirner, (CERN 96-01, Genève, 1996) Vol. 1, p. 141, *hep–ph/9602352*.

[2] W. Beenakker *et al.*, in *Physics at LEP2*, eds. G. Altarelli, T. Sjöstrand and F. Zwirner, (CERN 96-01, Genève, 1996) Vol. 1, p. 79, *hep–ph/9602351*.

[3] G. Gounaris *et al.*, in *Physics at LEP2*, eds. G. Altarelli, T. Sjöstrand and F. Zwirner, (CERN 96-01, Genève, 1996) Vol. 1, p. 525, *hep–ph/9601233*.

[4] E. Accomando *et al.*, *Phys. Rept.* **299** (1998) 1.

[5] E.N. Argyres *et al.*, *Phys. Lett.* **B358** (1995) 339.

[6] W. Beenakker *et al.*, *Nucl. Phys.* **B500** (1997) 255.

[7] R.G. Stuart, *Phys. Lett.* **B262** (1991) 113;
A. Aeppli, G.J. van Oldenborgh and D. Wyler, *Nucl. Phys.* **B428** (1994) 126.

[8] W. Beenakker and A. Denner, *Int. J. Mod. Phys.* **A9** (1994) 4837.

[9] M. Böhm, A. Denner and S. Dittmaier, *Nucl. Phys.* **B376** (1992) 29.

[10] A. Denner, S. Dittmaier and G. Weiglein, *Nucl. Phys.* **B440** (1995) 95 and references therein.

[11] A. Denner and S. Dittmaier, *Phys. Rev.* **D54** (1996) 4499.

[12] F.A. Berends and R. Kleiss, *Z. Phys.* **C27** (1985) 365.

[13] F.A. Berends et al., in *Z Physics at LEP1*, eds. G. Altarelli, R. Kleiss and C. Verzegnassi (CERN 89-08, Geneva, 1989), Vol. 1, p. 89.

[14] W. Beenakker, F.A. Berends and A.P. Chapovsky, *hep–ph/9805327*.

[15] W. Beenakker, F.A. Berends and S.C. van der Marck, *Z. Phys.* **C46** (1990) 687.

[16] V.S. Fadin, V.A. Khoze and A.D. Martin, *Phys. Rev.* **D49** (1994) 2247 and *Phys. Lett.* **B320** (1994) 141.

[17] K. Melnikov and O. Yakovlev, *Phys. Lett.* **B324** (1994) 217.

[18] K. Melnikov and O. Yakovlev, *Nucl. Phys.* **B471** (1996) 90.

[19] W. Beenakker, A.P. Chapovsky and F.A. Berends, *Phys. Lett.* **B411** (1997) 203 and *Nucl. Phys.* **B508** (1997) 17.

[20] A. Denner, S. Dittmaier and M. Roth, *Nucl. Phys.* **B519** (1998) 39.

[21] A. Denner, S. Dittmaier and M. Roth, *Phys. Lett.* **B429** (1998) 145.